

Parameter Optimization of 1-D Multi-FM SSD on the NIF

Aaron M. Van Dyne

Laboratory for Laser Energetics, University of Rochester, 250 East River Road, Rochester, New York 14623

Abstract

This work investigates the parameters that affect 1-D Multiple Frequency Modulation (Multi-FM) Smoothing by Spectral Dispersion (SSD) on the National Ignition Facility and demonstrates that a high level of uniformity can be achieved using Multi-FM by employing an optimization procedure. The laser non-uniformity that directly drives an inertial confinement fusion target can imprint on the target's shell during the ablation process, leading to the exponential growth of non-uniformity leading to the shell's destruction. The SSD system mitigates imprint by causing the speckle pattern to evolve continuously, creating many statistically independent patterns that average over time. The 1-D Multi-FM SSD system uses multiple phase modulators with different frequencies in a single dimension. A MATLAB program was developed to optimize 1-D Multi-FM SSD by intelligently varying the parameters to minimize a metric based on time integrated laser non-uniformity and laser system constraints. The MATLAB program's algorithm is based on the Levenberg-Marquadt method to find optimal solutions based on local derivative values. The MATLAB program was able to produce realizations of 1-D Multi-FM SSD that have lower levels of non-uniformity compared to single modulator designs. The OMEGA-EP laser will be used as a test bed for the new designs.

1. Introduction

The laser systems known as OMEGA¹ and the National Ignition Facility (NIF)² require a high degree of laser-beam uniformity to perform direct-drive inertial confinement fusion (ICF)^{3,4} experiments. Laser non-uniformity seeds the Rayleigh-Taylor hydrodynamic instability, which consequently degrades performance.⁵⁻¹¹ OMEGA and the NIF employ various techniques to improve on-target irradiation uniformity and reduce the laser imprint on direct-drive target designs, such as smoothing by spectral dispersion (SSD)¹²⁻¹⁵ and continuous phase plates.^{16,17} The non-uniformity in the lower spatial frequencies is the most problematic because hydrodynamic instabilities can develop during their longer imprinting periods, and these frequencies are hardest to smooth with SSD.

Continuous phase plates offer control over the far-field intensity envelope even in the presence of typical laser system phase aberrations. High spatial frequency non-uniformity, known as speckle¹⁸, is a direct consequence of phase plates. To lessen the effect of this speckle,

SSD is employed, which smoothes the speckle on a time scale shorter than the target can respond hydrodynamically. SSD achieves this effect by continuously altering the speckle pattern over time. The time-integrated far-field spot ends up being sufficiently uniform for ICF experiments when the SSD system has sufficient bandwidth and divergence. The SSD system can be applied in orthogonal spatial dimensions: 1-D SSD alters the speckle in one spatial dimension, and 2-D SSD alters it in two spatial dimensions. Multiple frequency modulation (Multi-FM) SSD employs multiple phase modulators in the direction of modulation and provides increased flexibility in smoothing performance. Standard 1-D SSD, which refers to the traditional process with only a single modulator, is limited to one or two color cycles due to a coherent interference effect similar to that of a double slit.¹⁹ A color cycle is one cycle through all of the phases within the beam. For example, in a 1 color cycle system, each color would appear once in a color contour plot of near-field phase. Multi-FM employs many color cycles over many modulators which tends to mitigate this interference effect. Multi-FM 1-D SSD uses only 500 GHz of bandwidth as opposed to the 900 GHz of bandwidth for standard 1-D SSD, defined as one leg of the 2-D system originally proposed for the NIF, which used 17 GHz, 2 color cycles, and 100 μ rad of full-angle divergence. The reduced applied bandwidth implies that only a single frequency tripling crystal is necessary²⁰ as opposed to the two necessary for standard 1-D SSD. Multi-FM 1-D SSD, which offers numerous benefits over standard 1-D SSD, will be the focus of this work.

2. Optics and the Fourier transform

In optics there are two important regions: the near field and far field as seen in Figure 1. The near field is the region before the beam has passed through the lens, and the far field is the region near the focal plane of the lens. Based on Fourier optics, the far-field image is the Fourier

transform of the near-field image²¹. The Fourier transform is a mathematical operation that can be applied to any well-behaved function of any number of variables, eg. time and space. The Fourier transform of a continuous time-dependent function transforms it into a continuous spectrum of frequencies²². The equation representing a formal temporal transform is given by,

$$F(\omega) = \int_{-\infty}^{\infty} f(t) e^{i\omega t} dt \quad (1)$$

where $f(t)$ a function of time t , ω is an angular frequency, and $F(\omega)$ is the Fourier transform of $f(t)$. The equation for a 1-D spatial transform in the x -direction is given by,

$$F(k_x) = \int_{-\infty}^{\infty} f(x) e^{-ik_x x} dx \quad (2)$$

where $f(x)$ is a function of location in the x direction, k_x is a spatial frequency, and $F(k_x)$ is the Fourier transform of $f(x)$. The Fourier transform operators are used to examine the effect of smoothing in the far field.

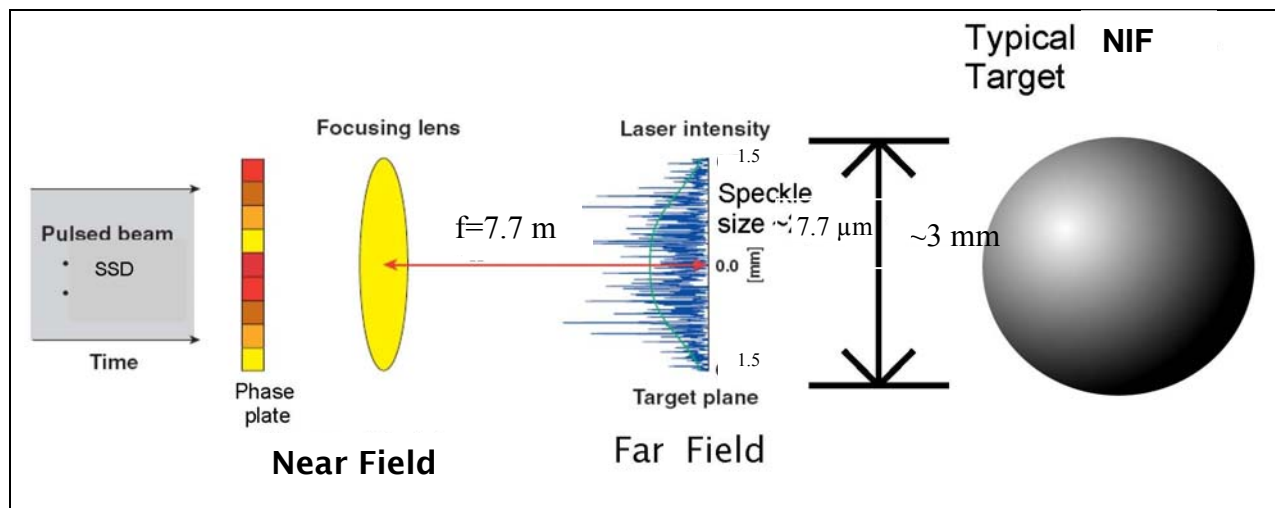


FIG. 1 A diagram showing the near field and far field for the NIF. The near field is the region before the lens, and the far field is the region near the focal plane of the lens. The phase plate shapes the beam to contain 95% of the enclosed energy in 3 mm, which slightly overfills the 3 mm target. The speckle size is on the order of $7.7\ \mu\text{m}$. This value comes from the equation $d=f\lambda/D$ where d is the speckle size, f is the focal length, D is the diameter of the beam, and λ is the wavelength of the light. For the NIF, $f=7.7\text{ m}$, $D=35.1\text{ cm}$, and λ is 351 nm .

3. Diffractive Optics

A diffractive optic known as a continuous phase plate is used to shape the far-field spot. This results in high spatial frequency artifacts, called speckle. This high spatial frequency speckle can be smoothed effectively by thermal conduction in the plasma around the NIF target unlike long-wavelength non-uniformity. The phase plate causes speckle because the beam is coherent. If a perfect beam passes through a lens, a diffraction limited spot is created in the far field. The width of this spot is defined as the distance from the center to the first zero and is determined by the equation $d=f\lambda/D$, where d is the spot size, f is the focal length of the lens, λ is the wavelength of the laser, and D is diameter of the beam or lens (whichever is smaller). For the NIF, the focal length is 7.7 m , the diameter is 35.1 cm , and the wavelength is 351 nm . This yields a spot size of $7.7\ \mu\text{m}$, but with the addition of phase aberration, this spot grows. When a strong phase aberration is added, such as that of the phase plate which makes the spot 400 times larger, the far field spot simply can be thought of as being many copies of the same $7.7\ \mu\text{m}$ spot distributed over the far-field plane.

4. The necessity of uniformity

In order to achieve ignition the target must be compressed by the laser such that the mixture of deuterium and tritium reaches a sufficiently high temperature and pressure. Uniform compression of the target is necessary to achieve this combination of temperature and pressure. This uniform compression requires a laser with a high level of uniformity. Hydrodynamic simulations show that ignition can be achieved using 1-D Multi-FM SSD, but further research could allow more flexibility in target and pulse shape choice. The 1-D Multi-FM smoothing system offers very promising options for achieving ignition. The system smoothes effectively and offers other benefits. These benefits include the feasibility of implementing the system in fiber optics as opposed to the bulk optics necessary for 2-D SSD. The Multi-FM system also requires only a single frequency tripling crystal.

5. SSD

The spot in the far field must be large enough to fill the 3 mm diameter target used on the NIF. There are two methods that can be employed: defocusing the far-field spot and employing a diffractive phase plate to shape the far-field spot. Each of these options has different consequences. The target can be placed outside of the focal plane creating a defocused spot as can be seen in figure 2a, but this creates a static long-wavelength non-uniformity that cannot be smoothed. The other option is to shape the spot using an engineered continuous phase element called a phase plate²³ that controls all the low spatial wavelengths that govern the overall spot shape. As previously mentioned, this results in high-frequency non-uniformity, known as speckle, figure 2b. Fortunately speckle can be smoothed. The method of smoothing used on OMEGA and the NIF is SSD, which involves continuously changing the speckle pattern to create many statistically independent random speckle patterns over time. The smoothing then occurs via

the temporal averaging of the independent patterns over time. This temporal averaging is possible because the speckle pattern changes faster than the target can respond hydrodynamically. The net laser non-uniformity imprinted on the target is reduced because the target reacts to a smoother spot. A version of SSD referred to as 1-D SSD involves the alteration of the speckle pattern in one spatial dimension, and as a result, there are striations in the far-field spot depicted in figure 2c. These striations are not seen in the far-field spot for 2-D SSD because this smoothing scheme alters the speckle pattern in two spatial dimensions. While 2-D SSD does yield a superior non-uniformity, 1-D SSD can be improved by using Multi-FM. It has been shown that employing the Multi-FM smoothing scheme is sufficient to achieve ignition²⁴. The 1-D SSD system also offers certain advantages because it can be done in a fiber and requires only a single frequency tripling crystal whereas 2-D SSD requires bulk optics and two frequency tripling crystals because for equivalent smoothing 2-D SSD requires more bandwidth.

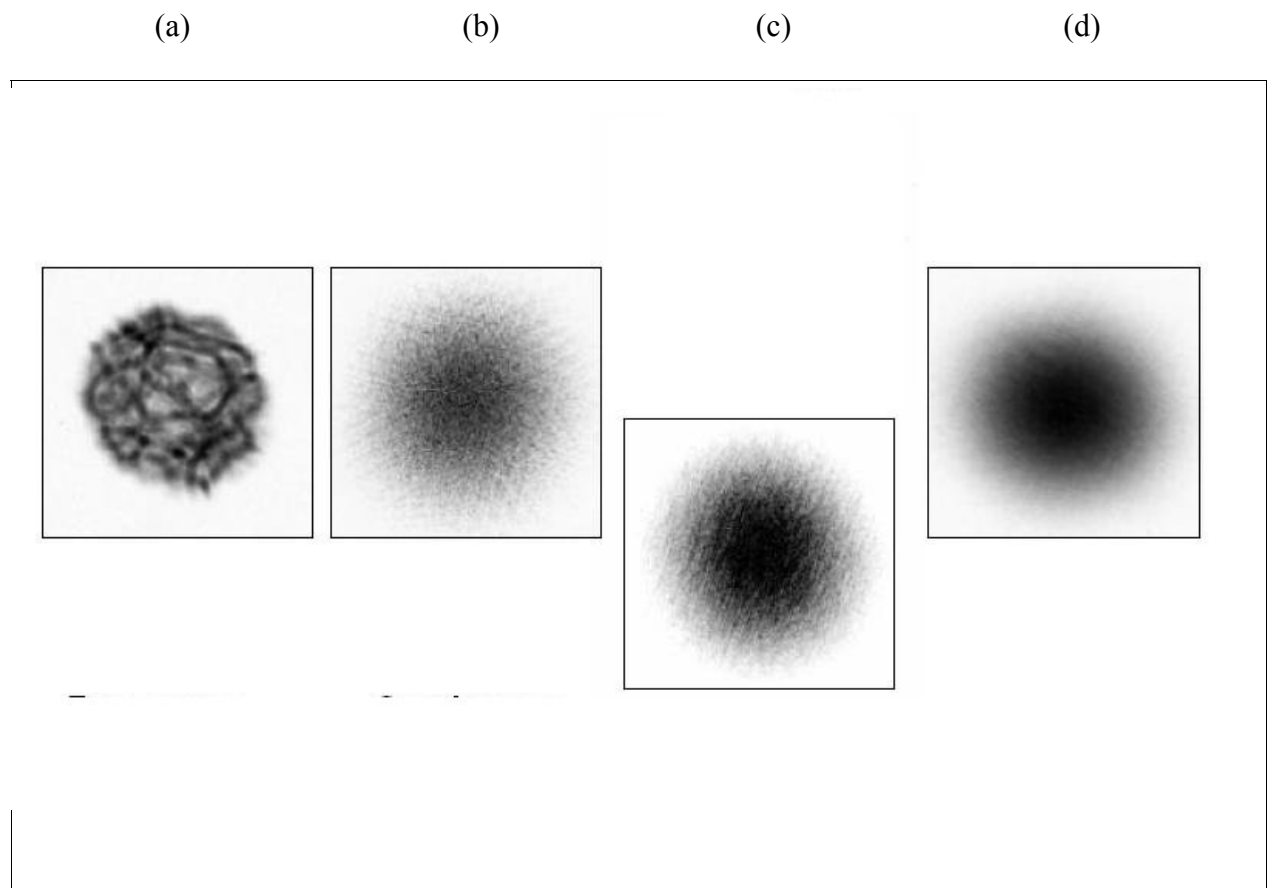
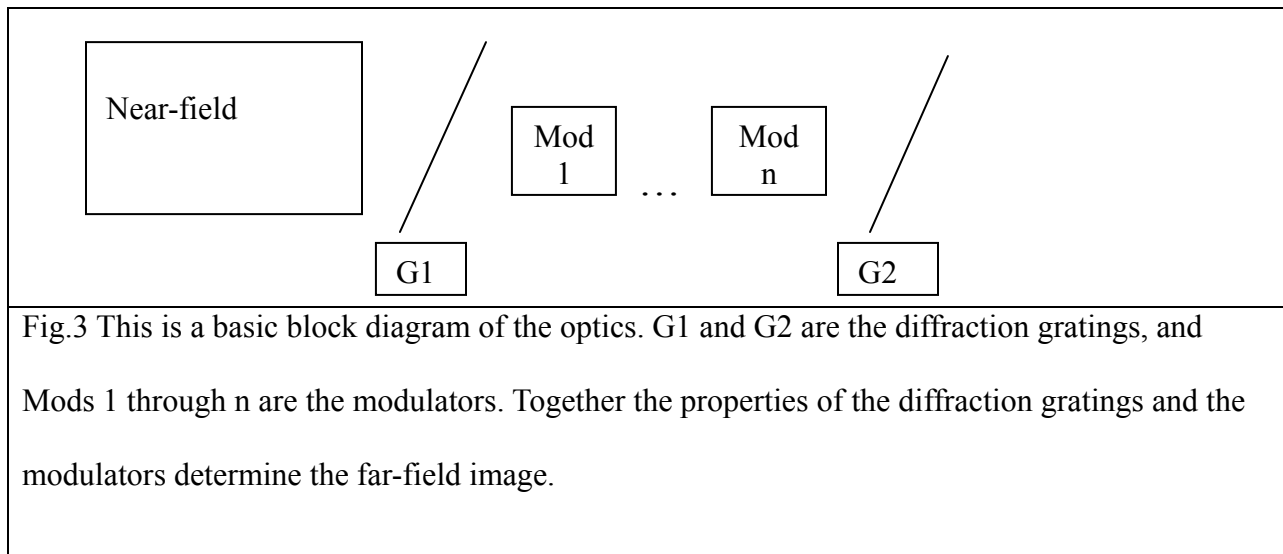


FIG.2 Far field spots for various techniques of illuminating the whole target and smoothing the beam. a) Defocused spot, target outside of focal plane with long-wavelength non-uniformity. b) Time-integrated far-field shaped by phase plate with high-frequency speckle. c) Time-integrated far-field spot with 1-D SSD applied. The striations are visible. d) Time-integrated far-field spot with 2-D SSD applied. There are no longer striations visible in the far-field spot.

6. Multi-FM

An alternative smoothing option denoted as 1-D Multi-FM SSD involves the use of multiple phase modulators in a single spatial dimension. There are two independent parameters involved in any form of FM for each modulator: modulation frequency and bandwidth. The grating dispersion is also an independent parameter of the system as a whole. The gratings and

modulators are shown in a block diagram of the optics, figure 3. Other important parameters can be derived from these parameters such as angular divergence, which is the spread in the far field. Certain constraints must be placed on any SSD system based on physical limitations of high-power laser systems: bandwidth and divergence. The bandwidth needs to be less than 500 GHz due to the pass band of a single frequency tripling crystal, and the angular divergence has to be less than 250 μrad due to the smallest pinhole in the NIF laser chain. It is also important that the modulation depth (a measure of how much each modulator's frequency varies) be greater than one in order to yield a side-peaked distribution,²⁵ which is better for uniformly irradiating the target. The proposed 1-D Multi-FM SSD system employs the benefit of multiple color cycles. Standard 1-D SSD is limited to one or two color cycles, figure 4a, due to a coherent interference effect similar to a double slit experiment. This interference effect results in a loss of smoothing at the resonances. The proposed 1-D Multi-FM SSD system takes advantage of multiple color cycles as can be seen in figure 4b. The colors are arranged in a quasi-random pattern of phase where the colors are out of synchronization with each other. It is this effect of having the separations of identical colors vary over time that mitigates the resonant effect.



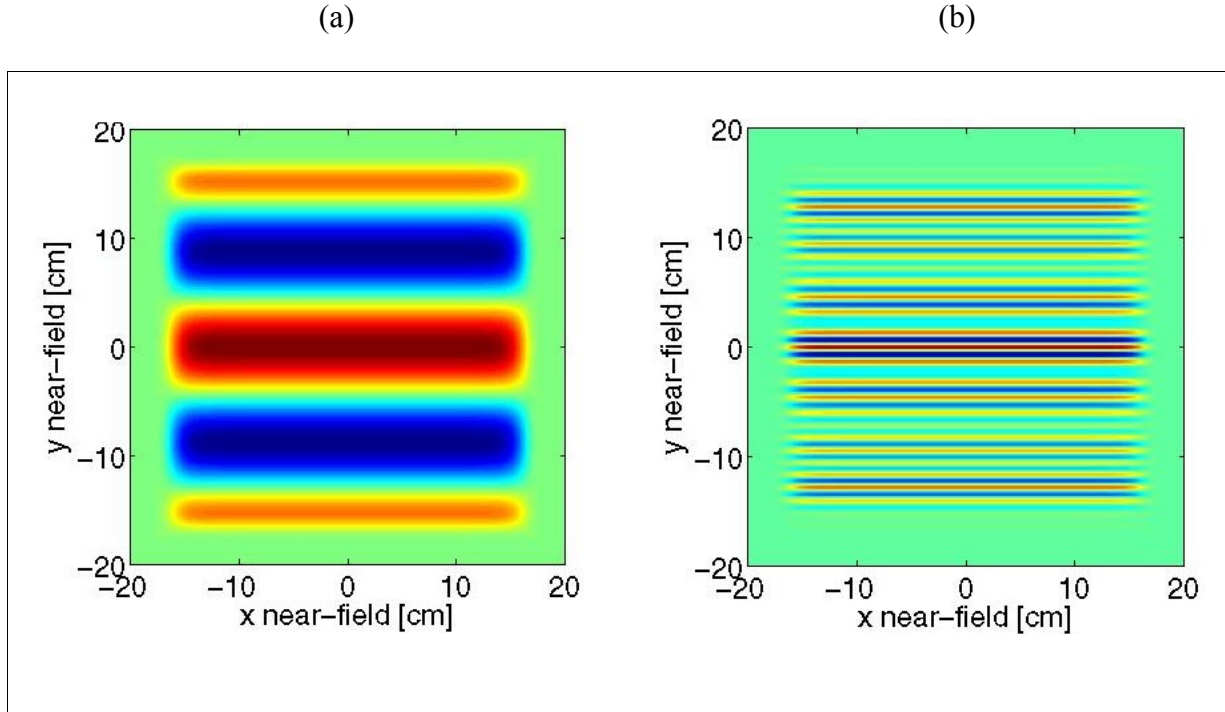


FIG. 4 Two similar color contour plots of phase in terms of x near-field and y near-field spatial coordinates. a) The plot illustrates Standard 1-D SSD with 2 color cycles. In this system the colors are in synchronization with each other creating an interference effect that causes a loss of smoothing at the resonances. b) The plot illustrates the fact that the Multi-FM system makes use of multiple color cycles and the colors are arranged in a quasi-random pattern. The colors in this system are not in synchronization, which mitigates the interference effect.

7. The code for optimizing the parameters

The optimization of a multi-variable function employs a metric that measures the overall effects of each parameter. The metric used in this work allows the effect of each parameter on the far-field non-uniformity to be evaluated. A code that optimizes the parameters was developed in MATLAB and is called, `Loop_analyzeMultiFM`. The code `Loop_analyzeMultiFM` controls another MATLAB code called `analyzeMultiFM`, which calculates certain values in the far field based on the SSD parameters. The code `Loop_analyzeMultiFM` alters various SSD parameters: the number of modulators, the frequency of each modulator, and the number of color cycles and modulation depths of each modulator. The code `analyze_MultiFM` then calculates certain values

such as the bandwidth, angular divergence, and asymptotic non-uniformity. After the parameters are optimized, the code also generates diagnostic plots of the far field in terms of divergence and bandwidth, a color contour plot of the phase in the near field, and the asymptotic non-uniformity in terms of the dimensionless spatial wave number l defined as $l \equiv kr$ where $k = 2\pi/\lambda$, λ = the spatial wavelength, and r = the target radius. The code `Loop_analyzeMultiFM` was written to vary the parameters that are fed to `analyzeMultiFM` in an intelligent manner. The parameters are the number of modulators and the frequencies, and the coefficients that help determine the number of color cycles and modulation depth of each modulator; eg. a total of 9 parameters when the number of modulators is 4. Based on these inputs, `analyzeMultiFM` determines bandwidth, modulation depth, the number of color cycles, temporal shear, as well as other values in the far field such as angular divergence and asymptotic non-uniformity. The temporal shear is how much the beam is offset in the temporal dimension by the optics.

The diagnostic outputs from `analyzeMultiFM` are combined to create a performance metric that attempts to limit far-field non-uniformity within realistic constraints. The performance metric is denoted as σ . These realistic constraints include: limiting the bandwidth, temporal shear, and angular divergence. The bandwidth has to be less than 500 GHz because of the frequency tripling crystals. The angular divergence has to be less than 250 μrad because of the smallest pinhole size in the NIF laser chain, and the temporal shear has to be less than 350 ps in order to not limit the pulse's rise time. It is preferable for the modulation depth to be greater than one because this prevents a highly center-peaked distribution. Three different ranges for the non-uniformity are used: the asymptotic non-uniformity over l -modes 60 to 80, l -modes 20 to 100, and l -modes 20 to 600. Each of the individual values that contribute to the metric has to be scaled, so that the resultant values are of a similar magnitude (referred to as

normalization). Each of these normalized terms is represented by β , which is used to develop sigma by the equation $\text{sigma}=\beta*\alpha$, where α determines the relative weight of each value. First the asymptotic non-uniformities are divided by the number of l-modes in their respective ranges. The asymptotic non-uniformities are then multiplied by a normalizing factor. The asymptotic non-uniformity over l-modes 60 to 80 is multiplied by 8,000. The asymptotic non-uniformity over l-modes 20 to 100 is multiplied by 20,000, and the asymptotic non-uniformity over l-modes 20-600 is multiplied by 36,680. The modulation depth, bandwidth, temporal shear, and angular divergence parts of the metric are normalized using the equation

$$\beta=e^{(\zeta-\gamma)/\chi} \quad (3)$$

where β is the normalized value, and χ , γ , ζ are values specific to the parameter. This method is used to keep the metric low as long as the parameter is within the physical limit but cause it to skyrocket if the parameter exceeds the physical limit. For the modulation depth ζ is 1.5, γ is the modulation depth, and χ is 1. These values were chosen in an effort to force the modulation depth to be greater than 1. For the bandwidth ζ is the bandwidth, γ is 500 GHz, and χ is 100GHz. For the divergence, ζ is the divergence, γ is 300 μrad , and χ is 100 μrad . These values were chosen in an effort to limit the divergence to being less than 250 μrad . For the temporal shear, ζ is the temporal shear, γ is 400 ps, and χ is 100 ps. This was chosen in an effort to force the temporal shear to be less than 350 ps. It was observed that the algorithm attempts to make some of the physical parameters much lower or higher than γ or ζ , the value modifying them, in order to achieve a very low sigma. Therefore, it may be noted that the γ or ζ used to modify the physical parameters are sometimes greater than the actual physical constraints. By making the modifying values larger than the actual constraint, the parameter gets much closer to the level that it is being constrained from crossing. This effect is important because in the case of the bandwidth, angular

divergence, and temporal shear, the best results are seen as the values grow larger, and the constraint exists because of a physical constraint of the laser system. The values ζ , γ , and χ can continue to be changed in the future to fine tune the algorithm.

In order to use β to develop sigma, the β values are weighted, to adjust the relative importance of each parameter. The weightings, α , chosen have a substantial impact on the optimal solutions that are found, so many combinations of weightings were tested to see which worked best. For example, if not enough weight is placed on the modulation depth, it begins to go substantially below 1. The majority of the weight has to be placed on the asymptotic level from l-modes 60 to 80 because these modes have been the most problematic in hydrodynamic simulations²³. The asymptotic non-uniformity over l-modes 60 to 80 has an α of 10, the asymptotic non-uniformity over l-modes 20 to 100 has an α of 5, the asymptotic non-uniformity over l-modes 20 to 600 has an α of 2, the modulation depth has an α of 6, the bandwidth has an α of 4, the angular divergence has an α of 3, and the temporal shear has an α of 3.

The actual algorithm used in the code Loop_analyzeMultiFM is based on the Levenberg-Marquardt method¹⁶, which uses local partial derivatives to determine how the free parameters should be varied. This algorithm varies one parameter at a time, and changes it by 5 percent until the derivative of sigma with respect to the parameter becomes positive, then goes back to the value that yielded the lowest sigma and changes it by 5 percent at a time in the other direction. The algorithm stops changing the parameters if sigma stops changing, the value of the parameter returns to the value that yielded the lowest sigma after the parameter has changed 5 times, or the value of the parameter exceeds limits placed on the parameter. The code then moves to the next free parameter and alters it. The code alters each of the free parameters in this cycle three times. The cycle is repeated because there is a non-linear relationship between the

parameters, so the parameters must be optimized based on the optimal values of the other parameters. It is also for this reason that the first parameter optimized is the coefficient for the number of color cycles, which was observed to be the most sensitive, and the last parameter to be optimized is the maximum modulation frequency, which was observed to be the least sensitive.

8. An Optimized Multi-FM System

An optimized 1-D Multi-FM SSD system with 500 GHz of bandwidth outperforms a standard 1-D SSD system with 900 GHz of bandwidth and is comparable to a full 2-D SSD system with 1 THz of bandwidth, and as a result, only a single frequency tripling crystal is necessary as opposed to the three necessary for standard 1-D SSD. An optimized system found by the code contains four modulators each defined by the previously discussed two independent parameters and the diffraction grating. Each modulator has a frequency between 25 and 50 GHz, a number of color cycles between 10 and 18, and all the indicators of bandwidth indicate a bandwidth just under 500 GHz. One measure of bandwidth is the correlation-width bandwidth, which is given by the following equation,

$$\text{Correlation-width bandwidth} = \frac{[\int F(\omega)d\omega]^2}{\int [F(\omega)]^2 d\omega} \quad (4)$$

where $F(\omega)$ is the function representing the pulse and ω is the frequency. The correlation-width bandwidth was by far the lowest of the measures of bandwidth because the wings of the function aren't equally weighted for center-peaked distributions. This fact caused an issue because the correlation-width divergence indicated a divergence well below 250 μrad full angle.

Unfortunately, the spread seen in figure 5, a plot of the far-field intensity in terms of divergence, appears to have too much intensity beyond the levels allowed by the pinhole. To rectify this, a different metric for divergence might be used in the future although this might be unnecessary if future optimal systems are more side-peaked. This center-peaked distribution is a result of low

modulation depths, which ranged from 0.6 to 1.1 for the modulators in this system. It was found that modulation depths over 1 smooth better and yield more side-peaked distributions. The other issue with this system is that its temporal shear is about 400 ps. This is an anomaly within the algorithm that must be worked out in the future because a temporal shear of greater than 350 ps limits the risetime of the pulse.

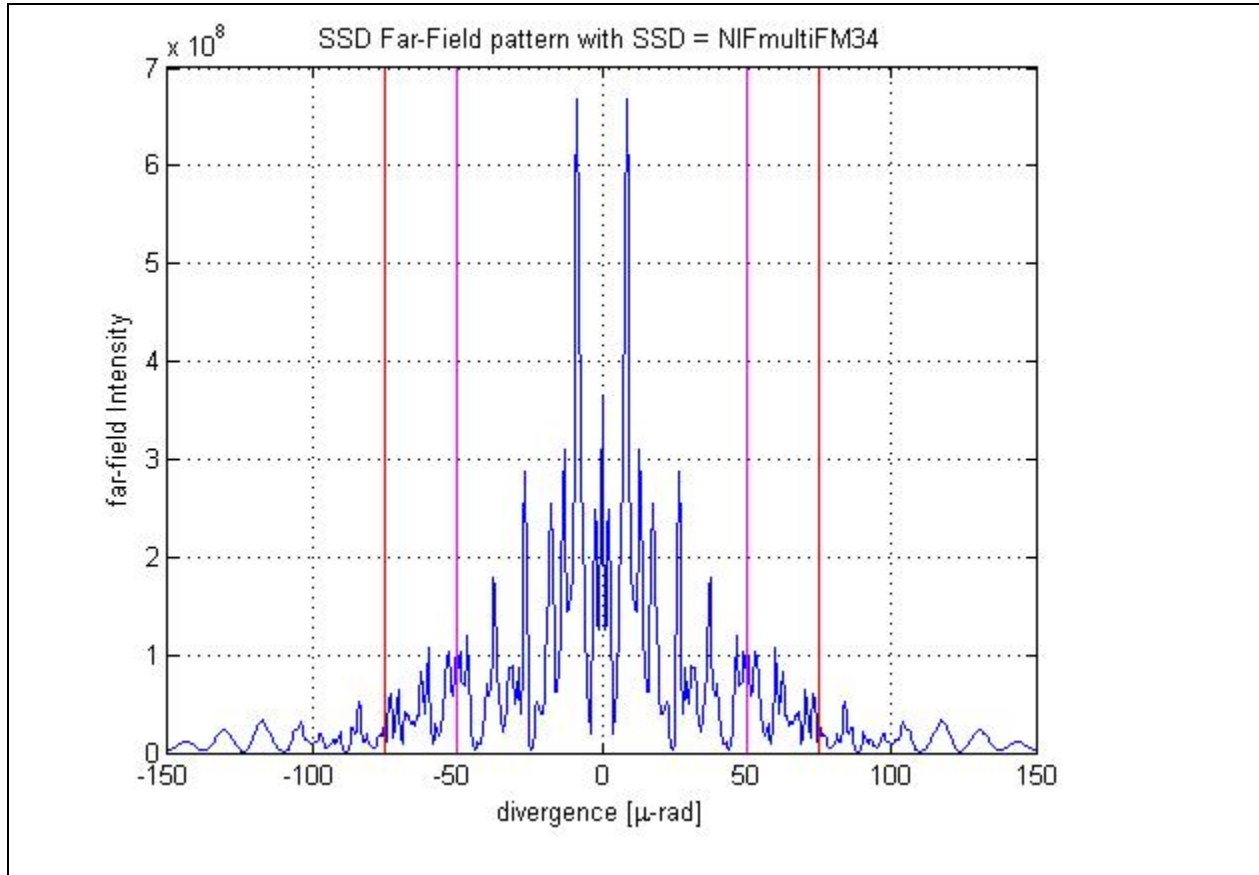
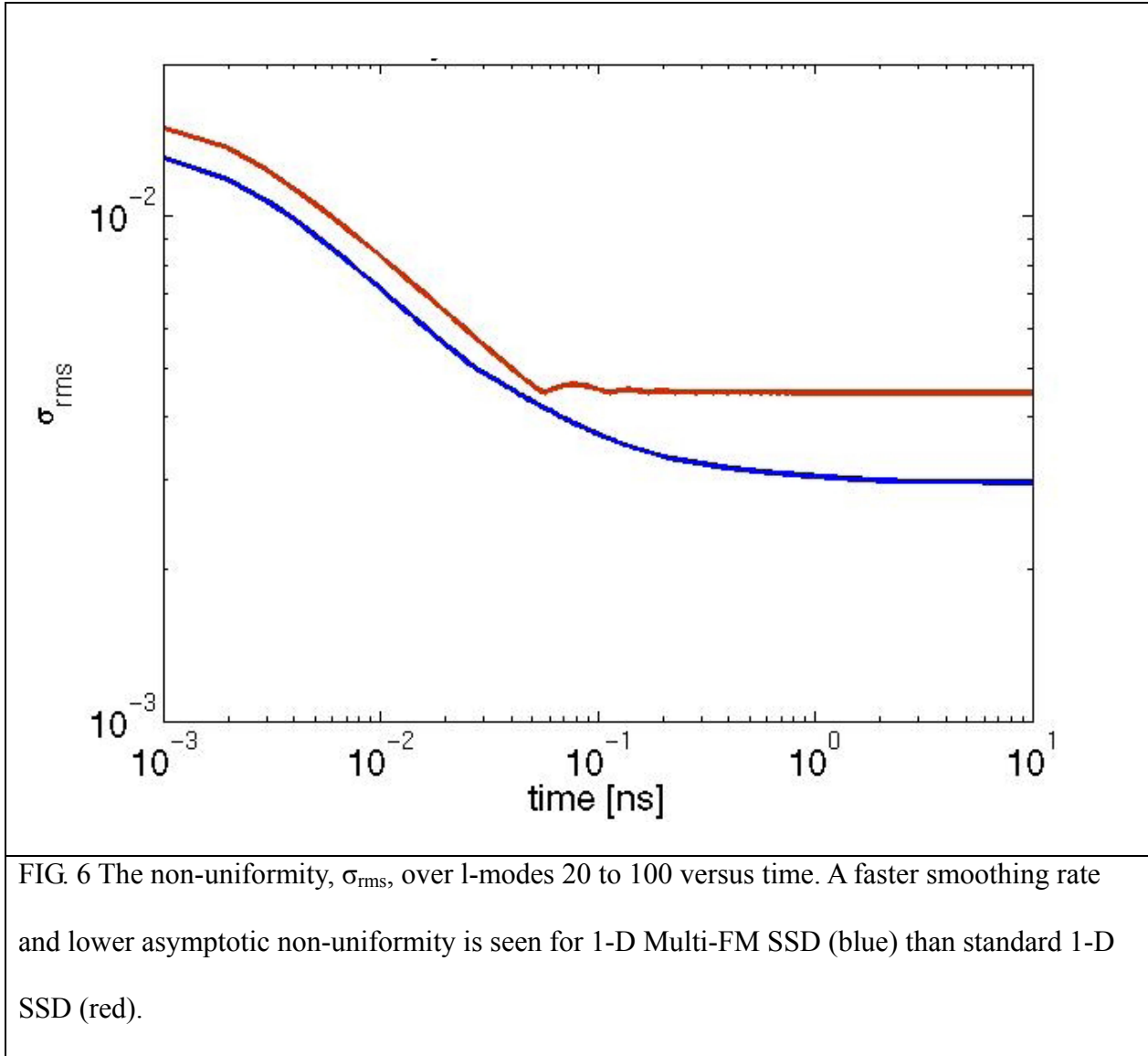


FIG. 5 Plot of far-field intensity vs. angular divergence. The far-field intensity does not flatten out sufficiently at the edges of the plot. At 125 μrad the far-field intensity must be almost zero in order to avoid encountering problems with the pinhole.

There are two ways of representing the far-field performance of an SSD system: the non-uniformity over time and the asymptotic non-uniformity versus l-mode. In both cases 1-D Multi-FM SSD outperforms standard 1-D SSD. A plot of the σ_{rms} non-uniformity over l-modes 20 to 100 versus time, figure 6, demonstrates a higher smoothing rate and lower asymptotic non-

uniformity for Multi-FM 1-D SSD than standard 1-D SSD.



Similarly, figure 7, a plot of asymptotic non-uniformity versus l-mode, demonstrates a lower asymptotic non-uniformity for all l-modes for Multi-FM 1-D SSD. It is important to note that the plot of asymptotic non-uniformity is over l-modes 2 to 600 whereas the plot of non-uniformity versus time is only over l-modes 20 through 100. This is because l-modes greater than 100 have low decoupling times, which means that the laser has hydrodynamically decoupled from the

target at that modal range, and that modal range is not affected as much by non-uniformity after this time, and l-modes less than 20 are not impacted as much by SSD, so the l-modes that were likely to be the most important are used in figure 7.

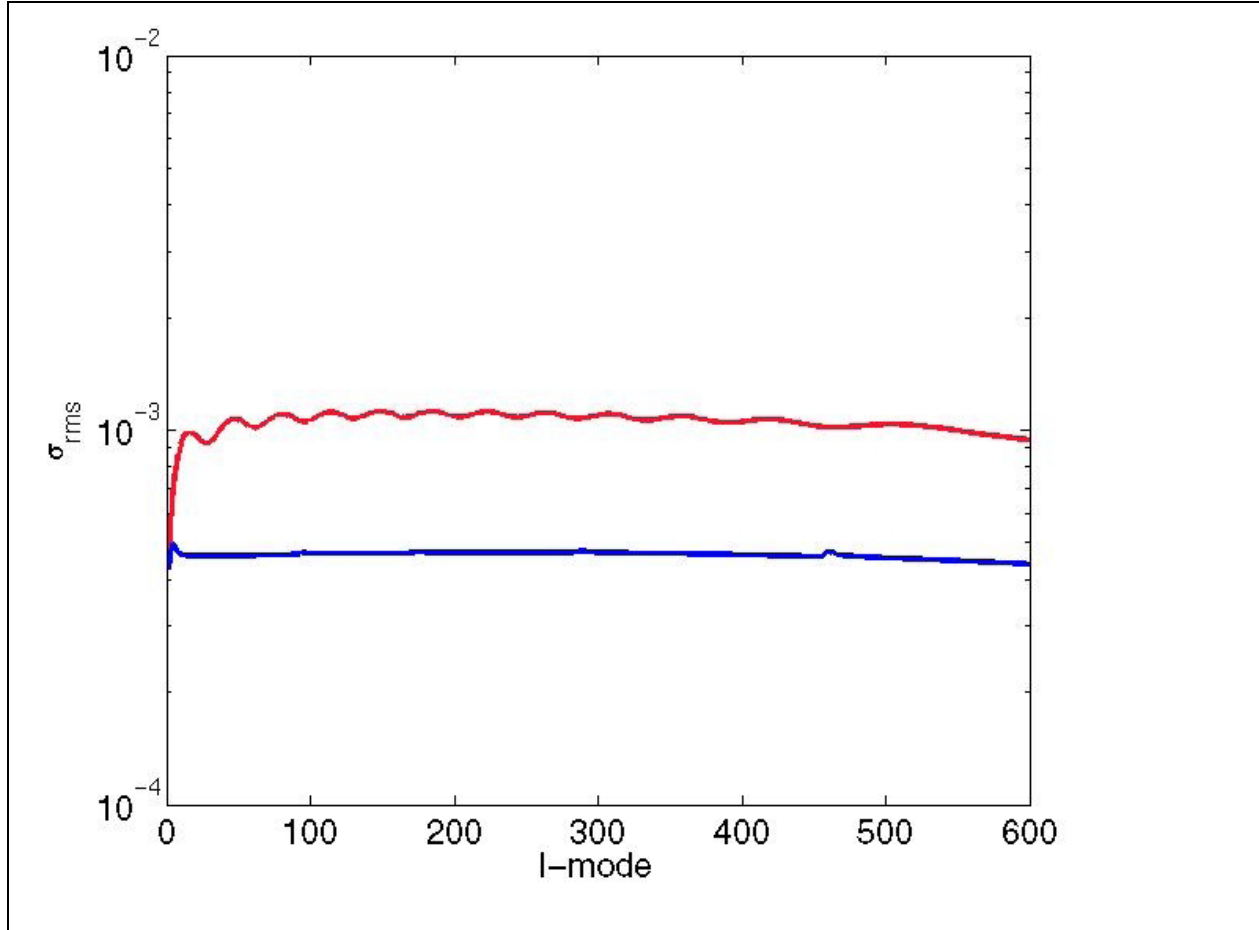


FIG.7 Plot of asymptotic non-uniformity versus l-mode. For all l-modes 1-D Multi-FM SSD (blue) has a lower asymptotic non-uniformity than standard 1-D SSD (red). More consistent smoothing over all the l-modes is also seen.

9. Conclusion

An optimized Multi-FM system with 500 GHz of bandwidth outperforms standard, single modulator, 1-D SSD with 900 GHz of bandwidth and is comparable to a 2-D SSD system with 1 THz of bandwidth.²⁴ This 1-D Multi FM system involves 4 modulators defined by several parameters. Each modulator has between 10 and 18 color cycles, a frequency between 25 and 50 GHz, and modulation depths between 0.6 and 1. In the future, it would be desirable to have

modulation depths greater than 1 because this will yield a more side-peaked distribution. The bandwidth was right around the maximum 500 GHz. The correlation-width measure of divergence indicates a value less than 250 μ rad, but inspection of a plot of far-field intensity versus deviation indicates otherwise. For this reason, a new measure of divergence is necessary, although the current measure may be satisfactory for more side-peaked distributions. The temporal shear was around 400 ps, which is greater than the desired limit of 350 ps, because the code consistently indicated that optimal solutions had a temporal shear of this magnitude in spite of attempts to limit it. When too much limitation was employed, the temporal shear dropped too low. This is an issue that must be worked out in the future. Multi-FM 1-D SSD is a promising concept, and Loop_analyzeMultiFM generated an optimal solution that demonstrates this in hydrodynamic simulations.²⁴

Acknowledgements

This project was completed during the Summer High School Internship program through the University of Rochester's Laboratory for Laser Energetics. This program was run by Dr. R.S. Craxton, and the project was completed with the supervision and aid of Dr. John Marozas. The Laboratory for Laser Energetics is supported by the United States Department of Energy Office of Confinement Fusion.

References

1. T. R. Boehly, D. L. Brown, R. S. Craxton, R. L. Keck, J. P. Knauer, J. H. Kelly, T. J. Kessler, S. A. Kumpman, S. V. J. Loucks, S. A. Letzring, F. J. Marshall, R. L. McCrory, S. F. B. Morse, W. Seka, J. M. Soures, and C. P. Verdon, "Initial performance results of the OMEGA laser system," *Opt. Commun.* **133**, 495-506 (1997).

2. J. Paisner, J. D. Boyes, S. A. Kumpman, W. H. Lowdermilk, and M. S. Sorem, “National Ignition Facility would boost US industrial competitiveness,” *Laser Focus World* **30**, 75-77 (1994).
3. C. P. Verdon, “High-performance direct-drive capsule designs for the National Ignition Facility,” *Bull. Am. Phys. Soc.* **38**, 2010 (1993).
4. S. E. Bodner, D. G. Colombant, J. H. Gardner, R. H. Lehmborg, S. P. Obenschain, L. Phillips, A. J. Schmitt, J. D. Sethian, R. L. McCrory, W. Seka, C. P. Verdon, J. P. Knauer, B. B. Afeyan, and H. T. Powell, “Direct-drive laser fusion: status and prospects,” *Phys. Plasmas* **5**, 1901–1918 (1998).
5. D. K. Bradley, J. A. Delettrez, and C. P. Verdon, “Measurements of the effect of laser beam smoothing on direct-drive inertial-confinement-fusion capsule implosions,” *Phys. Rev. Lett.* **68**, 2774–2777 (1992).
6. J. Delettrez, D. K. Bradley, and C. P. Verdon, “The role of the Rayleigh–Taylor instability in laser-driven burnthrough experiments,” *Phys. Plasmas* **1**, 2342–2349 (1994).
7. J. D. Kilkenny, S. G. Glendinning, S. W. Haan, B. A. Hammel, J. D. Lindl, D. Munro, B. A. Remington, S. V. Weber, J. P. Knauer, and C. P. Verdon, “A review of the ablative stabilization of the Rayleigh–Taylor instability in regimes relevant to inertial confinement fusion,” *Phys. Plasmas* **1**, 1379–1389 (1994).
8. R. Epstein, “Reduction of time-averaged irradiation speckle nonuniformity in laser-driven plasmas due to target ablation,” *J. Appl. Phys.* **82**, 2123–2139 (1997).
9. V. A. Smalyuk, T. R. Boehly, D. K. Bradley, V. N. Goncharov, J. A. Delettrez, J. P. Knauer, D. D. Meyerhofer, D. Oron, and D. Shvarts, “Saturation of the Rayleigh–Taylor growth of broad-bandwidth laser-imposed nonuniformities in planar targets,” *Phys. Rev. Lett.* **81**,

5342–5345 (1998).

10. F. J. Marshall and G. R. Bennett, “A high-energy x-ray microscope for inertial confinement fusion,” *Rev. Sci. Instrum.* **70**, 617–619 (1999).

11. F. J. Marshall, J. A. Delettrez, V. Yu. Glebov, R. P. J. Town, B. Yaakobi, R. L. Kremens, and M. Cable, “Direct-drive, hollow-shell implosion studies on the 60-beam, UV OMEGA laser system,” *Phys. Plasmas* **7**, 1006–1013 (2000).

12. S. Skupsky, R. W. Short, T. Kessler, R. S. Craxton, S. Letzring, and J. M. Soures, “Improved laser-beam uniformity using the angular dispersion of frequency modulated light,” *J. Appl. Phys.* **66**, 3456–3462 (1989).

13. S. Skupsky and R. S. Craxton, “Irradiation uniformity for high-compression laser-fusion experiments,” *Phys. Plasmas* **6**, 2157–2163 (1999).

14. J. E. Rothenberg, “Comparison of beam-smoothing methods for direct-drive inertial confinement fusion,” *J. Opt. Soc. Am. B* **14**, 1664–1671 (1997).

15. S. P. Regan, J. A. Marozas, J. H. Kelly, T. R. Boehly, W. R. Donaldson, P. A. Jaanimagi, R. L. Keck, T. J. Kessler, D. D. Meyerhofer, W. Seka, S. Skupsky, and V. A. Smalyuk, “Experimental investigation of smoothing by spectral dispersion,” *J. Opt. Soc. Am. B* **17**, 1483–1489 (2000).

16. T. J. Kessler, Y. Lin, J. J. Armstrong, and B. Velazquez, “Phase conversion of lasers with low-loss distributed phase plates,” in *Laser Coherence Control: Technology and Applications*, H. T. Powell and T. J. Kessler, eds., Proc. SPIE 1870, 95–104 (1993).

17. Y. Lin, T. J. Kessler, and G. N. Lawrence, “Design of continuous surface-relief phase plates by surface-based simulated annealing to achieve control of focal-plane irradiance,” *Opt. Lett.* **21**, 1703–1705 (1996).

18. J. W. Goodman, "Statistical properties of laser speckle patterns," in Laser Speckle and Related Phenomena, J. C. Dainty, ed., Vol. 9 of Topics in Applied Physics (Springer-Verlag, 1984), Chap. 2.
19. David Halliday, Robert Resnick and Jearl Walker, Fundamentals of Physics 540-542 (Wiley, 2004).
20. A. Babushkin, R.S. Craxton, S. Oskoui, M.J.Guardalmen, R.L. Kreck, and W. Seka, "Demonstration of the dual-tripler scheme for increased-bandwidth third-harmonic generation," Opt. Lett. **23**, 927-929 (1998)
21. J. W. Goodman, Introduction to Fourier Optics (McGraw-Hill, 1988).
22. R.N. Bracewell, "The Fourier Transform and Its Applications", 1986.
23. John A. Marozas, "Fourier transform-based continuous phase plate design technique: a high-pass phase-plate design as an application for OMEGA and the National Ignition Facility," J. Opt. Soc. Am. **A24**, 74-83 (2007).
24. Advisor, Dr. John Marozas, hydrodynamic simulations of a NIF scale ignition target generated based on 1-D Multi-FM SSD parameters described in this work.
25. A. B. Carlson, Communication Systems: An Introduction to Signals and Noise in Electrical Communication, McGraw- Hill Electrical and Electronic Engineering Series (McGraw-Hill, 1968) pp. 153–154.